Ferromagnetic Nickel(II) Polynuclear Complexes with End-On Azido as Bridging Ligand. The First Nickel(II)–Azido One-Dimensional Ferromagnetic Systems

Joan Ribas,*[1a] Montserrat Monfort,[1a] Carmen Diaz,[1a] Carles Bastos,[1a] and Xavier Solans[1b]

Departament de Química Inorgànica, Universitat de Barcelona, Diagonal 647, 08028-Barcelona, Spain and Departament de Cristal.lografia i Mineralogia, Universitat de Barcelona, Martí i Franqués, s/n, 08028-Barcelona, Spain

Received July 28, 1993[⊗]

Four new nickel(II) polynuclear end-on azide-bridged compounds: $[\{Ni(en)_2\}_2(\mu\text{-}N_3)_2](ClO_4)_2$ (**1**), $[\{Ni(en)(\mu\text{-}N_3)_2\}_n]$ (**2**), $[\{Ni(tn)(\mu\text{-}N_3)_2\}_n]$ (**3**), and $[\{Ni(Me_2tn)(\mu\text{-}N_3)_2\}_n]$ (**4**) were synthesized and characterized; en is ethylenediamine, tn is 1,3-diaminopropane, and Me_2tn is 2,2′-dimethyl-1,3-diaminopropane. The crystal structures of **1**, **2**, and **3** have been solved. Complex **1** crystallizes in the monoclinic system, space group $P2_1/n$, with fw = 640.76, a = 8.450(1) Å, b = 13.234(2) Å, c = 11.750(2) Å, β = 103.67(1)°, V = 1276.7 Å^3, Z = 2, R = 0.060, and R_w = 0.063. Complex **2** crystallizes in the triclinic system, space group $P\bar{1}$, with fw = 202.51, a = 16.675(6) Å, b = 12.458(4) Å, c = 5.538(2) Å, α = 98.84(2)°, β = 90.04(3)°, γ = 108.67(4)°, V = 1075(1) Å^3, Z = 3, R = 0.066, and R_w = 0.066. Complex **3** crystallizes in the monoclinic system, space group $P2_1/c$, with fw = 216.9, a = 12.956(5) Å, b = 22.408(7) Å, c = 5.695(3) Å, β = 103.82(3)°, V = 1605.(2), Z = 8, and R = 0.112. In the three complexes, the nickel atom is placed in a distorted octahedral environment: in complex **1** each nickel(II) is surrounded by two ethylenediamine ligands and two bridging end-on azido ligands. In complexes **2** and **3** each nickel(II) is surrounded by only one amine (en or tn) and four bridging end-on azido ligands, giving a neutral stoichiometry. The Ni–Ni distances are 3.369 Å for **1**, 3.190 Å for **2**, and 3.312 Å for **3**. The magnetic properties of the four compounds have been studied by means of susceptibility measurements vs temperature. For the 1-D systems **2**–**4** magnetization measurements vs applied field, for several temperatures, have also been carried out. The $\chi_M T$ vs T plots for **1**–**4** show the typical shapes for ferromagnetically coupled nickel(II) polynuclear complexes. By using the spin Hamiltonian $-2J\sum S_i S_j$, J values for **1**–**4** were 21.7, 11.9, 19.8, and 16.9 cm^{-1}, respectively. Introducing the single-ion zero field splitting parameter (D) in the Hamiltonian causes J parameters to vary slightly but the accuracy of this paprameter is discussed. Magnetization measurements for **2** and **3** indicate long-range antiferromagnetic order at low temperatures (metamagnetism).

Introduction

The azido anion is a versatile bridging ligand which can coordinate Ni(II) ions, giving dinuclear complexes in either end-to-end[2-5] or end-on[6-9] form, tetranuclear complexes in end-on[10] form, 1–D complexes in end-to-end form (uniform chains[11-13] and alternating chains[14]), and, finally, bidimensional complexes in which both end-to-end and end-on forms are present.[15] Surprisingly, no one-dimensional Ni(II) ferromagnetic system with an azido bridging ligand has been reported to date. Taking into account that ferromagnetic coupling in these systems is caused by the end-on azido bridging ligand[16] and that these ferromagnetic systems always have two bridging ligands, it could be expected that for the synthesis of these new ferromagnetic 1D systems, four of the coordination sites on each nickel(II) should be occupied by four azido bridging ligands and only two coordination sites would be free to link to the other terminal ligand: the stoichiometry of these 1D complexes should be $[Ni(N_3)_{4/2}(amine)]$. With this idea in mind we undertook the synthesis of the possible new complexes in a ratio Ni/amine/azido = 1/1/2, and we were able to prepare and characterize the three new 1-D complexes here presented, working with different bidentate amines: $[\{Ni(en)(\mu\text{-}N_3)_2\}]_n$ (**2**), $[\{Ni(tn)(\mu\text{-}N_3)_2\}]_n$ (**3**), and $[\{Ni(Me_2tn)(\mu\text{-}N_3)_2\}]_n$ (**4**) where en = ethylenediamine, tn = 1,3-diaminepropane, and Me_2tn = 2,2′-dimethyl-1,3-diaminopropane. The structure of two of these 1-D systems, with en and tn, has been solved. On the other hand during this work we realized not only that the Ni/amine/azido ratio was important but also that the counter anions used in the synthesis were not-innocent. Thus, working with ethylenediamine with 1/2/1 ratio two different complexes could be obtained: ClO_4^- as counter anion gives the new ferromagnetic dinuclear complex (**1**), and using PF_6^- as counter anion gives antiferromagnetically coupled dinuclear complex previously reported by us.[5] On the other hand, working with tn ligand and ClO_4^- as counter anion, the 1-D complex (**3**) is always obtained with either a 1/2/1 or a 1/1/2 ratio, but with BPh_4^- as counter anion, an antiferromagnetic dinuclear complex,

⊗ Abstract published in *Advance ACS Abstracts*, December 15, 1993.

(1) (a) Department of Inorganic Chemistry, University of Barcelona. (b) Department of Crystallography, University of Barcelona.
(2) Wagner, F.; Mocella, M. T.; D'Aniello, M. J.; Wang, A. J. H.; Barefield, E. K. *J. Am. Chem. Soc.* **1974**, *96*, 2625.
(3) Pierpont, C. G.; Hendrickson, D. N.; Duggan, D. M.; Wagner, F.; Barefield, E. K. *Inorg. Chem.* **1975**, *14*, 604.
(4) Chaudhuri, P.; Guttman, M.; Ventur, D.; Wieghardt, K.; Nuber, B.; Weiss, J. J. *J. Chem. Soc., Chem. commun.* **1985**, 1618.
(5) Ribas, J.; Monfort, M., Diaz, C., Bastos, C.; Solans, X. *Inorg. Chem.* **1993**, *32*, 3557.
(6) Arriortua, M. I.; Cortés, A. R.; Lezama, L.; Rojo, T.; Solans, X. *Inorg. Chim. Acta* **1990**, *174*, 263.
(7) Escuer, A.; Vicente, R.; Ribas, J. *J. Magn. Magn. Mater.* **1992**, *110*, 181.
(8) Vicente, R.; Escuer, E.; Ribas, J.; Fallah, M. S.; Solans, X.; Font-Bardía, M. *Inorg. Chem.* **1993**, *32*, 1920 and references therein.
(9) Cortés, R.; Ruis de Larramendi, J. I.; Lezama, L.; Rojo, T.; Urtiaga, K.; Arriortua, M. I. *J. Chem. Soc. Dalton Trans.* **1992**, 2723.
(10) Ribas, J.; Monfort, M.; Costa, R.; Solans, X. *Inorg. Chem.* **1993**, *32*, 695.
(11) Escuer, A., Vicente, R.; Ribas, J.; El Fallah, M. S.; Solans, X. *Inorg. Chem.* **1993**, *32*, 1033.
(12) Gadet, V.; Verdaguer, M.; Renard, J. P.; Ribas, J.; Monfort, M.; Diaz, C.; Solans, X.; Landee, C. P.; Lamet, J. P.; Dworkin, A. *J. Am. Chem. Soc.*, in press.
(13) Escuer, A.; Vicente, R., Ribas, J.; El Fallah, M. S.; Solans, X.; Font-Bardía, M. *Inorg. Chem.* **1993**, *32*, 3727.
(14) Vicente, R.; Escuer, A.; Ribas, J.; Solans, X. *Inorg. Chem.* **1992**, *31*, 1726.
(15) Monfort, M.; Ribas, J.; Solans, X. *J. Chem. Soc., Chem. Commun.* **1993**, 350.
(16) Charlot, M. F.; Kahn, O.; Chaillet, M.; Larrieu, C. *J. Am. Chem. Soc.* **1986**, *108*, 2574 and references therein.

0020-1669/94/1333-0484$04.50/0

previously reported,[5] is obtained. All these facts seem to indicate that further studies are necessary to be able to predict the kind of coordination and, indeed, the magnetic behavior.

Experimental Section

Caution! Perchlorate and azide complexes of metal ions are potentially explosive. Only a small amount of material should be prepared, and it should be handled with caution.

Synthesis of the New Complexes. $[\{Ni(en)_2\}_2(\mu\text{-}N_3)_2](ClO_4)_2$ (1). To an aqueous solution of 1 mmol (0.365 g) of $Ni(ClO_4)_2\cdot 6H_2O$ and 2 mmol (0.120 g) of ethylenediamine in 30 mL of water was added an aqueous solution of 1 mmol (0.065 g) of NaN_3. After filtration to avoid any impurity, the aqueous solutions were left undisturbed, and well-formed blue-dark crystals of **1** were obtained after several days.

$[\{Ni(en)(\mu\text{-}N_3)_2\}_n]$ (2). To an aqueous solution of 1 mmol (0.292 g) of $Ni(NO_3)_2\cdot 6H_2O$ and 1 mmol (0.065 g) of ethylenediamine in 30 mL of water was added an aqueous solution of 2 mmol (0.130 g) of NaN_3. After filtration to avoid any impurity, the aqueous solutions were left undisturbed, and well-formed blue crystals of **2** were obtained after several days.

$[\{Ni(tn)(\mu\text{-}N_3)_2\}_n]$ (3). (a) To an aqueous solution of 1 mmol (0.365 g) of $Ni(ClO_4)_2\cdot 6H_2O$ and 2 mmol (0.148 g) of 1,3-propanediamine in 30 mL of water was added an aqueous solution of 1 mmol (0.065 g) of NaN_3. After filtration to avoid any impurity, the aqueous solutions were left undisturbed and well-formed green crystals of **3** were obtained after several days. After a few more days, well-formed hexagonal blue crystals of $[\{Ni(tn)_2(\mu\text{-}N_3)\}_n](ClO_4)$ (NINAZ) were obtained.[12]

(b) To an aqueous solution of 1mmol (0.365 g) $Ni(ClO_4)_2\cdot 6H_2O$ and 1 mmol (0,074 g) of 1,3-propanediamine in 30 mL of water was added an aqueous solution of 2 mmol (0.130 g) of NaN_3. After filtration, a green microcrystalline powder of **3** was obtained after several days.

$[\{Ni(Me_2tn)(\mu\text{-}N_3)_2\}_n]$ (4). To an aqueous solution of 1 mmol (0.292 g) of $Ni(NO_3)_2\cdot 6H_2O$ and 1 mmol (0.162 g) of 2,2'-dimethyl-1,3-propanediamine in 30 mL of water was added an aqueous solution of 2 mmol (0.130 g) of NaN_3. A green microcrystalline powder of **4** immediately precipitated. All attempts to obtain good single crystals for X-ray structure determination were unsuccessful because when the mother liquor was left undisturbed for several days a new complex was obtained: the bidimensional $[Ni(N_3)_2(Me_2tn)]_n$ previously reported by us.[15] All attempts to recrystallize the 1-D complex (**4**) gave good crystals of the same 2D compound.[15] Satisfactory analytical results (C, H, N, Ni) were obtained for all complexes.

Physical Measurements. Magnetic measurements were carried out on polycrystalline samples with a pendulum type-magnetometer (MANICS DSM8) equipped with a helium continuous-flow cryostat working in the temperature range 300-4 K and a Brucker BE15 electromagnet. The magnetic field was approximately 15000 G. The instrument was calibrated by magnetization measurement of standard ferrite. Diamagnetic corrections were estimated from Pascal constants. Susceptibility measurements at low field (500, 1000 G) and magnetization measurements at low temperatures were carried out with a fully automatized SQUID spectrometer (Quantum Design) in the Laboratorie de Chimie de Coordination (Toulouse, France).

Crystal Data Collection and Refinement. Crystals (0.08 × 0.08 × 0.15) of **1**, (0.1 × 0.1 × 0.2 mm) of **2**, and (0.05 × 0.05 × 0.13) of **3** were selected and mounted on an ENRAF-NONIUS CAD4 four-circle diffractometer for 1 and on a Philips PW-1100 four-circle diffractometer for 2 and 3. Unit cell parameters were determined from automatic centering of 25 reflections ($16 \le \theta \le 21°$ for **1**, $8 \le \theta \le 12°$ for **2**, and $4 \le \theta \le 12°$ for **3** and refined by least-squares method. Intensities were collected with graphite-monochromatized Mo Kα radiation, using the $\omega/2\theta$ scan technique. For **1**, 3911 reflections were measured in the range $2 \le \theta \le 30°$, 3319 of which were assumed as observed applying the condition $I \ge 2.5\sigma(I)$. For **2**, 2123 reflections were measured in the range $2 \le \theta \le 25°$, 1328 of which were assumed as observed applying the same condition. For **3**, 2124 reflections were measured in the range $2 \le \theta \le 25°$, only 761 of which were assumed as observed applying the same condition. The small dimensions of crystals of **3** permitted the measurement of only a small number of reflections. Attempts with crystals from different crystallizations processes gave similar or poorer results. For this reason, all crystallographic results for **3** must be taken carefully. In the three compounds three reflections were measured every 2 h as orientation and intensity control, significant intensity decay was not observed. Lorentz–polarization corrections but not absorption corrections were made. The crystallographic data are shown in Table 1. The crystal structures were solved by Patterson synthesis using the SHELXS computer program[17] and refined by full-matrix least-squares methods, using the SHELX76[18] computer programs. The function minimized was $\sum w[|F_o| - |F_c|]^2$ where $w = [\sigma^2(F_o) + k|F_o|^2]^{-1}$ and $k = 0.011$ for 1, 0.0 for **2**, and 0.0348 for **3**. f, f', and f'' were taken from ref. 19. For **1** the positions of all H atoms were computed and refined with an overall isotropic temperature factor, using a riding model. For **3**, taking into account the considerations mentioned above and in order to refine the structure with an acceptable ratio of reflections/number of parameters, only Ni atoms were refined anisotropically. For **1** the final R factor was 0.060 (R_w = 0.063) for all observed reflections. The number of parameters refined was 155. Maximum shift/esd = 0.1; Maximum and minimum peaks in final difference synthesis were +0.3 and –0.3 e Å^{-3} respectively. For **2** the final R factor was 0.066 (R = 0.066) for all observed reflections. The number of parameters refined was 298. Maximum shift/esd = 0.1. Maximum and minimum peaks in final difference syntheses were again 0.5 and –0.5 e Å^{-3} respectively. Final atomic coordinates for **1–3** are given in Tables 2–4, respectively.

Table 1. Crystallographic Data for $[\{Ni(en)_2\}_2(\mu\text{-}N_3)_2](ClO_4)_2$ (**1**), $[\{Ni(en)(\mu\text{-}N_3)_2\}_n]$ (**2**), and $[\{Ni(tn)(\mu\text{-}N_3)_2\}_n]$ (**3**)

	1	**2**	**3**
formula	$C_8H_{32}Cl_2N_{14}Ni_2O_8$	$C_2H_8N_8Ni$	$C_3H_{10}N_8Ni$
fw	640.76	202.71	216.9
temp, K	298	298	298
space group	$P2_1/n$	$P\bar{1}$	$P2_1/c$
a, Å	8.450(1)	16.675(6)	12.956(5)
b, Å	13.234(2)	12.458(4)	22.408(7)
c, Å	11.750(2)	5.538(2)	5.695(3)
α, deg	90.00	98.84(2)	90.00
β, deg	103.67(1)	90.04(3)	103.82(3)
γ, deg	90.00	108.67(4)	90.00
V, Å^3	1276.7(6)	1075(1)	1606(2)
Z	2	3	8
λ(Mo Kα), Å	0.710 69	0.710 69	0.710 69
d_{calcd}, g cm^{-3}	1.666	1.879	1.794
μ(Mo Kα), cm^{-1}	17.42	26.46	
R^a	0.060	0.066	0.112
R_w^b	0.063	0.066	

^{a} $R = \sum||F_o| - |F_c||/\sum|F_o|$. ^{b} $R_w = [\sum w(|F_o| - |F_c|)^2/\sum w|F_o|^2]^{1/2}$.

Table 2. Final Atomic Coordinates (×10^4, Ni and Cl × 10^5) for $C_8H_{32}Cl_2N_{14}Ni_2O_8$ (**1**)

	x/a	y/b	z/c	B_{eq},^{a} Å^2
Ni	11415(3)	7466(2)	10378(2)	2.53(2)
Cl	64133(9)	–9765(6)	29735(7)	4.25(3)
N(1)	397(3)	–792(1)	675(2)	3.33(8)
N(2)	780(3)	–1568(2)	1174(2)	3.44(7)
N(3)	1083(5)	–2328(2)	1624(3)	6.50(15)
N(4)	3274(3)	581(2)	430(2)	3.76(8)
N(5)	1754(3)	2288(2)	979(2)	3.49(8)
N(6)	–745(3)	1068(2)	1871(2)	3.81(8)
N(7)	2420(3)	469(2)	2761(2)	3.94(9)
C(1)	4217(4)	1513(3)	663(3)	4.79(13)
C(2)	3051(4)	2386(2)	348(3)	4.70(13)
C(3)	–44(5)	1138(3)	3131(3)	4.94(14)
C(4)	1241(5)	332(3)	3466(3)	5.52(15)
O(1)	6394(6)	18(4)	3447(6)	5.51(22)
O(2)	4818(4)	–1240(3)	2286(4)	4.38(16)
O(3)	7596(7)	–996(4)	2287(5)	5.83(25)
O(4)	6804(7)	–1669(4)	3912(4)	5.90(22)

^{a} ($B_{eq} = 8\pi^2/3U_{ij}a_i^*a_j^*a_ia_j$).

Results and Discussion

Description of the Structures. $[\{Ni(en)_2\}_2(\mu\text{-}N_3)_2](ClO_4)_2$ (1). The unit cell contains two dinuclear [NiNi] dications and four perchlorate anions. Selected bond lengths and angles are listed in Table 5. Other distances and angles may be found in the supplementary material. A view of the dinuclear unit with atom-

(17) Sheldrick, G. M. *Acta Crystallogr.* **1990**, *A46*, 467.
(18) Sheldrick, G. M. SHELX. A computer program for crystal structure determination. University of Cambridge, England, 1976.
(19) *International Tables for X-ray Crystallography*; Kynoch Press; Birmingham, England, 1976.

Table 3. Final Atomic Coordinates (×10⁴; Ni × 10⁵) for $(C_2H_8N_8Ni)_n$ (**2**)

	x/a	*y/b*	*z/c*	B_{eq},[a] Å²
Ni(1)	2222(4)	3663(6)	2562(12)	3.04(25)
Ni(2)	1205(3)	3017(5)	7294(10)	1.66(19)
Ni(3)	5536(3)	230(4)	2531(8)	0.87(16)
N(1)	2156(12)	2677(18)	4933(34)	2.02(74)
N(2)	2283(15)	1925(28)	4756(46)	3.43(125)
N(3)	2490(18)	807(24)	4528(64)	3.61(127)
N(4)	1046(11)	3777(17)	4253(39)	2.07(68)
N(5)	1052(21)	4865(39)	4033(60)	4.97(164)
N(6)	919(16)	5635(19)	4252(45)	2.91(101)
N(7)	2085(23)	4396(39)	9798(105)	6.61(220)
N(8)	1839(17)	5321(32)	9686(60)	3.91(136)
N(9)	1832(21)	6253(20)	393(49)	4.84(138)
N(10)	1296(14)	2240(19)	10061(42)	1.50(83)
N(11)	1031(23)	1342(28)	−81(47)	4.24(142)
N(12)	565(22)	302(21)	10533(68)	5.07(157)
N(13)	3177(16)	5179(22)	4032(46)	1.83(89)
N(14)	3061(18)	3262(35)	735(59)	4.22(148)
N(15)	57(14)	3289(18)	8731(48)	1.89(80)
N(16)	−280(29)	−1630(41)	−5207(101)	7.48(267)
N(17)	4622(12)	858(19)	4362(40)	1.90(77)
N(18)	4428(16)	1585(23)	4731(43)	2.21(88)
N(19)	4399(19)	12258(44)	5517(98)	6.53(211)
N(20)	4680(21)	−1173(24)	609(44)	2.30(98)
N(21)	4525(21)	−2107(25)	265(68)	3.34(134)
N(22)	4186(27)	7228(79)	140(81)	14.48(395)
N(23)	3385(18)	170(29)	−948(65)	3.31(112)
N(24)	3651(20)	−1716(23)	5357(42)	2.12(100)
C(1)	3923(32)	5043(32)	4564(75)	3.89(155)
C(2)	3951(19)	4371(25)	1412(57)	1.72(97)
C(3)	−634(20)	2131(32)	8157(65)	3.03(135)
C(4)	541(28)	−1763(37)	−6208(76)	3.43(164)
C(5)	2681(48)	9290(44)	8891(71)	10.55(315)
C(6)	2682(18)	−1469(35)	−4168(69)	3.79(144)

[a] $(B_{eq} = 8\pi^2/3U_{ij}a_i^*a_j^*a_ia_j)$.

Table 4. Final Atomic Coordinates (×10⁴) for $(C_3H_{10}N_8Ni)_n$ (**3**)

	x/a	*y/b*	*z/c*	B_{eq},[a] Å²
NiA	−38(1)	375(1)	2484(3)	1.19(6)
NiB	4711(1)	2875(1)	3419(2)	1.50(7)
N(1)A	688(9)	335(4)	−259(18)	2.98(32)
N(2)A	1761(9)	463(4)	−84(17)	2.98(32)
N(3)A	2568(8)	620(4)	−273(17)	2.98(32)
N(4)A	876(9)	−246(4)	4895(19)	2.82(31)
N(5)A	1896(9)	−339(4)	4948(17)	2.82(31)
N(6)A	2743(9)	−423(3)	4987(18)	2.82(31)
N(7)A	−1070(8)	983(4)	309(16)	2.76(24)
C(8)A	−1406(10)	1538(4)	1612(18)	2.76(24)
C(9)A	−414(9)	1882(5)	2717(18)	2.76(24)
C(10)A	353(9)	1610(4)	5132(18)	2.76(24)
N(11)A	883(8)	1071(4)	4223(15)	2.76(24)
N(1)B	3793(8)	2202(4)	1081(15)	2.48(26)
N(2)B	2961(7)	2078(4)	1105(15)	2.48(26)
N(3)B	2126(8)	1951(3)	1234(15)	2.48(26)
N(4)B	5637(10)	2777(4)	907(18)	2.71(28)
N(5)B	6477(9)	2895(4)	660(16)	2.71(28)
N(6)B	7344(8)	3024(3)	869(15)	2.71(28)
N(7)B	3742(8)	3556(4)	1622(15)	2.76(25)
C(8)B	4266(9)	4068(5)	650(18)	2.76(25)
C(9)B	4936(9)	4406(5)	2984(17)	2.76(25)
C(10)B	5952(10)	4084(5)	4104(17)	2.76(25)
N(11)B	5629(8)	3505(3)	5535(16)	2.76(25)

[a] $(B_{eq} = 8\pi^2/3U_{ij}A_i^*A_j^*A_i.A_j)$.

labeling scheme and cell packing are presented in Figure 1. The nickel atom occupies a distorated octahedral environment, formed by two N atoms of the two azido bridging ligands and four N atoms of the two bidentate ethylenediamine ligands. The central core, $Ni(N_3)_2Ni$, important from the magnetic point of view, has an inversion center with two Ni–N(N_3) distances of 2.144(2) Å and the other two of 2.123(2) Å. The Ni–Ni distance is 3.369 Å. The Ni–N–Ni angles are 104.3(2)°.

$[\{Ni(en)(\mu\text{-}N_3)_2\}_n]$ (2). Perspective view of a trinuclear fragment of one of the chains is presented in Figure 2 with an

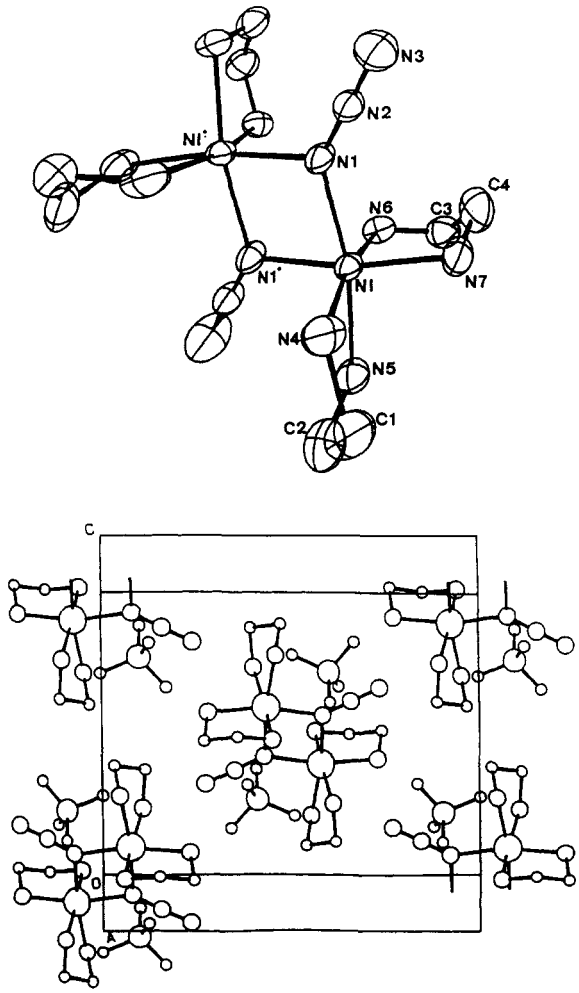

Figure 1. Labeling scheme (above) for the dinuclear cation and cell-packing diagram (below) of $[\{Ni(en)_2\}_2(\mu\text{-}N_3)_2](ClO_4)_2$ (**1**).

Table 5. Selected Bond Lengths (Å) and Angles (deg) for $C_8H_{32}Cl_2N_{14}Ni_2O_8$ (**1**)

N(1)–Ni	2.144(2)	N(7)–Ni	2.090(2)
N(1)i–Ni	2.123(2)	Ni···Ni(i)	3.369(1)
N(4)–Ni	2.101(2)	N(2)–N(1)	1.188(3)
N(5)–Ni	2.110(2)	N(3)–N(2)	1.138(3)
N(6)–Ni	2.102(2)		
N(4)–Ni–N(1)	93.9(1)	N(1)–Ni–N(1)i	75.7(1)
N(5)–Ni–N(1)	167.0(1)	N(4)–Ni–N(1)i	93.6(1)
N(5)–Ni–N(4)	81.6(1)	N(5)–Ni–N(1)i	92.4(1)
N(6)–Ni–N(1)	93.8(1)	N(6)–Ni–N(1)i	94.2(1)
N(6)–Ni–N(4)	170.2(1)	N(7)–Ni–N(1)i	169.7(1)
N(6)–Ni–N(5)	92.2(1)	Ni(i)–N(1)–Ni	104.3(2)
N(7)–Ni–N(1)	94.9(1)	N(2)–N(1)–Ni	133.6(2)
N(7)–Ni–N(4)	91.3(1)	N(2)–N(1)–Ni(i)	121.8(2)
N(7)–Ni–N(5)	97.3(1)	N(3)–N(2)–N(1)	177.0(3)
N(7)–Ni–N(6)	81.9(1)		

atom-labeling scheme. Main distances and bond angles are gathered in Table 6. Other distances and angles can be found in the supplementary material. The structure consists of two polymeric chains, which are not equivalent in crystal symmetry, of ethylenediamine–nickel(II) bridged by two azido ligands in a 1,1 coordination model. The chains run along the *c* axis. In the first chain (with Ni(3)) consecutive nickel(II) atoms are related by an inversion center, while in the second chain (with Ni(1) and Ni(2)) the two consecutive nickel atoms are not related by a crystallographic symmetry. The intrachain Ni–Ni distance is 3.190(7) Å. Each nickel(II) ion displays a distorted octahedral coordination, which is allowed by the small N–Ni–N bond angle of the inner ring Ni–N–Ni–N (77.3 and 81°). The $[Ni(N_3)_2(en)]$ repeat unit along the chain is neutral, and the closest

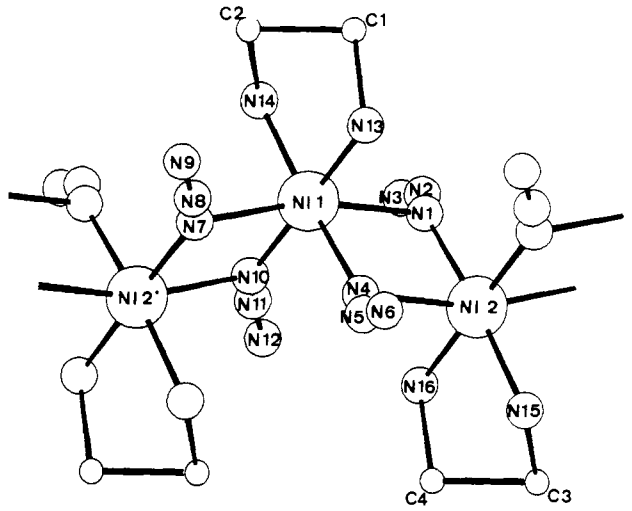

Figure 2. Perspective view of a trinuclear fragment and atom-labeling scheme of $[\{Ni(en)(\mu\text{-}N_3)_2\}_n]$ (**2**).

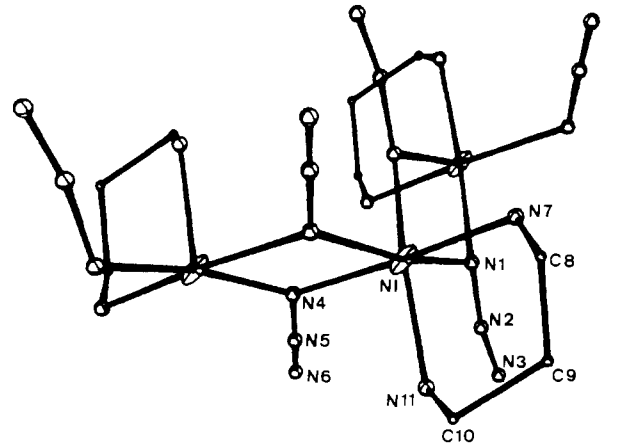

Figure 3. Perspective view of a trinuclear fragment and atom-labeling scheme of $[\{Ni(tn)(\mu\text{-}N_3)_2\}_n$ (**3**).

Table 6. Selected Bond Lengths (Å) and Angles (deg) for $(C_2H_8N_8Ni)_n$ (**2**)

	Unit A		
Ni(2)···Ni(1)	3.190(7)	N(1)–Ni(2)	2.16(2)
N(1)–Ni(1)	1.91(2)	N(4)–Ni(2)	2.11(2)
N(4)–Ni(1)	2.21(2)	N(7)–Ni(2)	2.16(4)
N(7)–Ni(1)	1.95(6)	N(10)–Ni(2)	1.96(2)
N(10)–Ni(1)	2.22(2)		
N(4)–Ni(1)–N(1)	81.1(10)	Ni(2)–N(1)–Ni(1)	103.(1)
N(10)–Ni(1)–N(7)	77.3(12)	Ni(2)–N(4)–Ni(1)	95.2(9)
N(4)–Ni(2)–N(1)	78.0(8)	Ni(2)–N(7)–Ni(1)	103(2)
N(10)–Ni(2)–N(7)	78.4(17)	Ni(2)–N(10)–Ni(1)	101(1)
	Unit B		
Ni(3)···Ni(3)	3.292(9)	N(20)–Ni(3)	2.01(3)
N(17)–Ni(3)	2.12(2)	N(20)i–Ni(3)	2.33(3)
N(17)i–Ni(3)	2.31(2)		
N(17)i–Ni(3)–N(17)	84.2(10)	N(20)i–Ni(3)–N(20)	85.4(10)

interchains are therefore short: N (azido, A)–N(azido, B) = 3.47 and 3.05 Å. No hydrogen bonds are present in the structure.

$[\{Ni(tn)(\mu\text{-}N_3)_2\}_n]$ (3). Perspective view of a trinuclear fragment of one of the chains is presented in Figure 3 with an atom labeling scheme. Main distances and bond angles are gathered in Table 7. Other distances and angles can be found in the supplementary material. The structure consists of two polymeric chains, which are not equivalent in crystal symmetry, of 1,3-propanediamine–nickel(II) bridged by two azido ligands in a 1,1-coordination mode. The chains run along the *c* axis. In the first chain (A), consecutive nickel(II) atoms are related by an inversion center, while in the second chain (B), they are related by a 2-fold helicoidal axis. In the first chain (A), the two nitrogen and the two nickel atoms of the ring Ni-N–Ni–N are chelated in pairs by an inversion center. In the second chain (B), the two nitrogen atoms are not related by crystallographic symmetry. The intrachain Ni-Ni distance is 3.31 Å. Each nickel(II) ion displays a distorted octahedral coordination, which is allowed by the small N–Ni–N bond angle of the inner ring Ni–N–Ni–N (71.9°). The $[Ni(N_3)_2(tn)]$ repeat unit along the chain is neutral and the closest interchains are therefore short: N(azido,A)–N(azido,B) = 3.21 Å; N(amine,A)–N(azido,B) = 3.24 Å. These values indicate that the possible N–H···N(azido) hydrogen bonds are weak.

Table 7. Selected Bond Lengths (Å) and Angles (deg) for $(C_3H_{10}N_8Ni)_n$ (**3**)[a]

unit	unit A	unit B
N(1)–Ni	2.009(10)	2.168(9)
N(1)*–Ni	2.082(10)	2.145(9)
N(4)–Ni	2.109(11)	2.087(12)
N(4)**–Ni	2.065(11)	2.185(12)
N(7)–Ni	2.093(10)	2.082(9)
N(11)–Ni	2.068(9)	2.044(9)
Ni–Ni	3.312(3)	3.307(1)
N(1)*–Ni–N(1)	71.9(4)	93.6(4)
N(4)–Ni–N(4)**	75.4(4)	93.3(4)
N(4)–Ni–N(1)	100.5(4)	78.4(4)
N(4)–Ni–N(1)*	88.6(4)	93.9(4)
N(1)–Ni–N(4)**	168.6(4)	169.2(3)
N(1)*–Ni–N(4)**	97.3(4)	80.0(4)
N(7)–Ni–N(1)	85.5(4)	92.1(4)
N(7)–Ni–N(4)	173.8(4)	169.2(4)
N(7)–Ni–N(1)*	91.6(4)	91.7(3)
N(7)–Ni–N(4)**	98.5(4)	96.8(4)
N(11)–Ni–N(7)	90.4(4)	88.9(4)
N(11)–Ni–N(1)	94.7(4)	89.0(4)
N(11)–Ni–N(4)	90.9(4)	85.8(4)
N(11)–Ni–N(1)*	166.2(4)	177.3(4)
N(11)–Ni–N(4)**	95.9(4)	97.3(4)
Ni*–N(1)–Ni	108.1(8)	100.1(9)
Ni**–N(4)–Ni	105.0(8)	101.4(10)

[a] Symmetry code: (*) unit a, $-x, -y, -z$; unit b, $x, {}^1/_2 - y, z + {}^1/_2$; (**) unit a, $-x, -y, 1 - z$; unit b, $x, {}^1/_2 - y, z - {}^1/_2$.

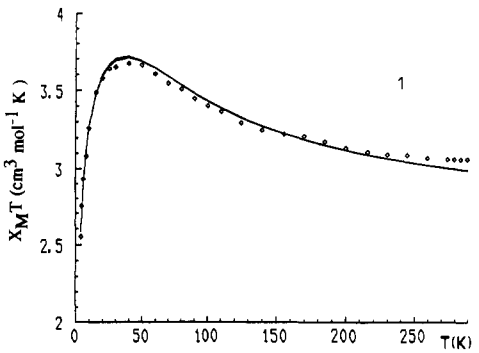

Figure 4. Experimental and calculated temperature dependence of $\chi_M T$ for $[\{Ni(en)_2\}_2(\mu\text{-}N_3)_2](ClO_4)_2$ (**1**).

Magnetic Properties. The $\chi_M T$ vs T plot for the dinuclear complex **1** is shown in Figure 4. The $\chi_M T$ values first increase, clearly indicating ferromagnetic behavior. At ca. 40 K a maximum is observed and then a continuous decrease up to 4 K, indicating the contribution of zero-field splitting, D, and antiferromagnetic coupling between the dinuclear entities. Variable-temperature susceptibility data (4–300 K) for **1** were analyzed using the isotropic Ginsberg model[20] from the Hamiltonian

$$H = -2JS_1S_2 - D({S_1}_z^2 + {S_2}_z^2) - g\beta H(S_1 + S_2) - z'J'S\langle S\rangle$$

in which J is the intradimer exchange parameter, D the single-ion

(20) Ginsberg, A. P.; Martin, R. L.; Brookes, R. W.; Sherwood, R. C. *Inorg. Chem.* **1972**, *11*, 2884.

Table 8. Best-Fit Magnetic Parameters for Compounds **1–4**

compound	J,[a] cm^{-1}	g	D, cm^{-1}	$z'J'$, cm^{-1}
1	20.9	2.31	0.35	−0.54
	21.7	2.30	0[b]	−0.37
2	14.8	2.27	−6.3	−1.27
	11.9	2.32	0[b]	−1.58
3	17.6	2.54	4.4	−1.07
	19.8	2.50	0[b]	−0.95
4	14.7	2.50	6.7	−1.28
	16.9	2.49	0[b]	−1.11

[a] From Hamiltonian $H = -2J\sum S_iS_j$. [b] D assumed to be zero (see text for explanation).

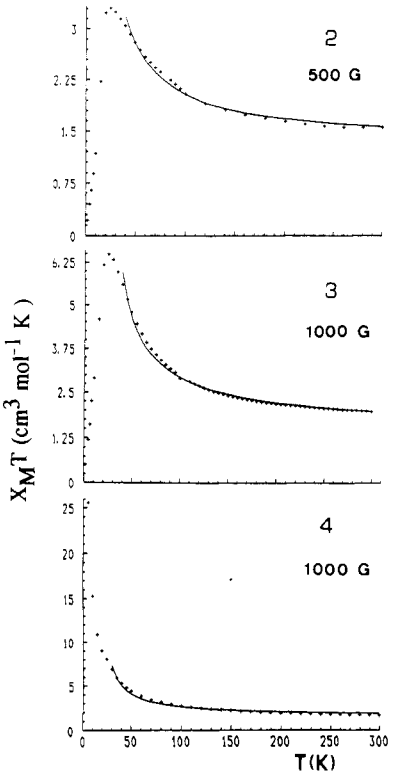

Figure 5. Experimental and calculated temperature dependence of $\chi_M T$ for $[\{Ni(en)(\mu\text{-}N_2)_2\}_n]$ (**2**), $[\{Ni(tn)(\mu\text{-}N_3)_2\}_n]$ (**3**), and $[\{Ni(Me_2tn)(\mu\text{-}N_3)_2\}_n$ (**4**).

zero-field splitting and $z'J'$ the quantity for effective interdimer exchange; it is assumed that $g_x = g_y = g_z = g$. Least-squares fitting of the magnetic data leads to the parameters reported in Table 8. The minimized function was $R = \sum(\chi_M^{calcd} - \chi_M^{obsd})^2/\sum(\chi_M^{obsd})^2$, and R was less than 10^{-4}. As previously indicated by Ginsberg,[20] the parameters D and $z'J'$ are very strongly correlated with each other, but are only weakly correlated with g and J. Thus, it is impossible to calculate the D and $z'J'$ values accurately. For this reason we have attempted to fit experimental results with the same Ginsberg formula but assuming $D = 0$ (as indicated by this author):[20] the magnetic parameters J, g, and $z'J'$ are very similar, and they are also reported in Table 8. The R factor (defined above) is as good as in the previous fitting. In Figure 4 both theoretical curves are put together and a good superposition is shown: only a small difference in the maximum zone (near 40 K) is observed. As a consequence we must assume that the two effects (D and $z'J'$) are present in our complexes at low temperature, but the values of the two variables are correlated, are very low, and do not influence the J or g values of **1**.

$\chi_M T$ measurements vs T for **2–4** are shown in Figure 5. The magnetic field in which these susceptibility measurements were made is given in the figure. Preliminary results with greater fields (1.5, 1.0 T) indicated a very strong dependence on external field in the low temperature region for 2 and 3. As previously pointed out,[21,22] such behavior is characteristic of the powder susceptibilities of metamagnetic systems. For this reason the susceptibility curves reported and fitted in this work are given at very low fields. Under these conditions (Figure 5), $\chi_M T$ products increase when the temperature decreases: this is the signature of a strong ferromagnetic interaction between Ni(II) ions within the chain. For **2**, $\chi_M T$ values vary from 1.6 (room temperature) to 3.3 cm^3 mol^{-1} K (25 K), and for **3**, these values vary from 2.2 (room temperature) to 6.4 cm^3 mol^{-1} K (25 K). These differences indicate stronger ferromagnetic coupling for **3** and different g values owing to different distortion in the idealized octahedral geometries around Ni(II). Below 25 K for **2** and **3**, a decrease of $\chi_M T$ is observed, which reveals an antiferromagnetic interaction between the chains (tridimensional antiferromagnetic ordering). For compound **4**, $\chi_M T$ values vary from 2 (room temperature) to 26 cm^3/mol^{-1} K (4 K) without any decrease at low temperature, indicating no antiferromagnetic ordering at any temperature higher than 4 K. From room temperature to 30 K the experimental data were fitted by the empirical relation proposed by de Neef[23] for the $S = 1$ ferromagnetic chains, using the Hamiltonian

$$H = -2J\sum(S_i \cdot S_{i+1}) - D\sum(S^2_{iz} - {}^2/_3) + g\beta H\sum S_{iz}$$

As indicated by de Neef, at low temperatures there is high uncertainty in the fitted parameters. The minimization of the agreement factor R leads to an intrachain coupling constant J_{intra}, which is collected in Table 8 together with g and D. It must be pointed out that, as indicated in the previous dinuclear system, the D parameter and the intermolecular $z'J'$ interaction are strongly correlated. In the de Neef formula these intermolecular interactions are not considered. Consequently, in these conditions attempts to determine the D values accurately appear difficult. For this reason we have applied the same de Neef formula assuming $D = 0$. The magnetic parameters do not show significant variation. These parameters are also included in Table 8. From $T_N \approx 25$ K for 2 and 3 (temperature of antiferromagnetic order) it is possible to compute an approximate value of the interchain interaction $J'_{inter} \approx -1.27$ cm^{-1} for 2 and −1.07 cm^{-1} for 3 from the following formula[24,25] in which z is the nearest neighboring chains:

$$kT_N = z|J_{intra}J'_{inter}|^{1/2}S^2$$

Since metamagnetic species have frequently been shown to exhibit sharp jumps in isothermal magnetizations,[26] we measured the magnetization at different temperatures in applied field up to 51 kG. The results are shown in Figure 6 for **2** and **3**, respectively, in which the normalized $M/N\beta$ vs H/T are represented. For **2** above 15 K, the experimental $M/N\beta$ values follow the Brillouin formula (solid line) indicating noninteracting entities in the 3-D net. The effective spin S value for Ni(II) was found to be greater than 1 because of the ferromagnetic interactions within the chains. The same behavior is observed for complex **3** but above 30 K, approximately. At low temperature (below 15 and 30 K respectively) the two complexes clearly separate from the solid line (Brillouin law) indicating strong antiferromagnetic interactions (metamagnetism). Without antiferromagnetic ordering all curves should be superposed to the solid line corresponding to the Brillouin formula. Then, the shape of the low-temperature curves, as previously reported for other ferromagnetic Ni(II) chains,[21,22,26] clearly indicates this antiferromagnetic ordering. In contrast, complex **4** presents a less pronounced deviation from the Brillouin formula even at very

(21) Witteveen H. T.; Rutten, W. L. C.; Reedijk, J. J. *Inorg. Nucl. Chem.* **1975**, *35*, 913.
(22) Estes, W. E.; Weller, R. R.; Hatfield, W. E. *Inorg. Chem.* **1980**, *19*, 26.
(23) De Neef, T. Ph.D. Thesis, Eindhoven, 1975.
(24) Renard, J. P.; Regnault, L. P.; Verdaguer, M. *Proc. Int. Cong. Magn., 1988, J. Phys. Colloq.* **1988**, *49*, 1425.
(25) Richards, P. M. *Phys. Rev.* **1974**, *B10*, 4687.
(26) Landau, D. P.; Keen, B. P.; Schneider, B and Wolf, W. P. *Phys. Rev. B* **1971**, *3*, 2310.

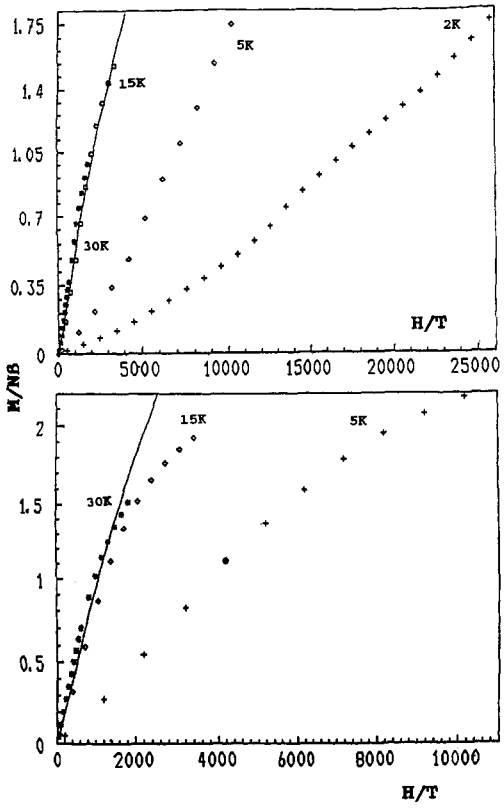

Figure 6. Magnetization isotherms ($M/N\beta$) vs H/T at different temperatures for [{Ni(en)(μ-N_3)$_2$}$_n$] (**2**) (above) and for [{Ni(tn)(μ-N_3)$_2$}$_n$] (**3**) (below).

low temperatures, in agreement with susceptibility measurements (no decrease of $\chi_M T$ values up to 4 K). This difference—in the absence of structural data of complex (**4**)—may be assumed to be due to the steric hindrances produced by the two CH_3 group in the amine chains, which prevent contact between nearer Ni(II) ferromagnetic chains.

Interpretation of the Magnetic Results. In ferromagnetic systems, attempts to relate the results with OM calculations, as in antiferromagnetic systems,[5] are not valid. Furthermore, in end-on azido complexes, the spin polarization effect must be taken into consideration. These Ni(II) systems are very similar to those reported by Kahn and co-workers for analogous Cu(II) systems.[16] Extended Hückel calculations demonstrate that, even if the gap between the magnetic orbitals is weak only for certain Cu–N–Cu angles giving the accidental orthogonality, the ferromagnetism is found for all angles and distances. This is the reason why Kahn develops the spin polarization concept as the key factor to explain the behavior of end-on azido bridges. In this theory the in-plane π_g orbital (HOMO) of N_3^- with a node on the central nitrogen atom is mainly considered. The electron of the bridging nitrogen atom (α spin, for example) is partially delocalized toward the two d_{xy} metal orbitals. Consequently, each unpaired electron of the two metal ions is likely to have β spin, which favors the triplet state. As a result, the coupling would ferromagnetic whatever the values of distances or angles.

Our results seem to indicate that this effect is also the predominant factor which explain the ferromagnetic behavior in Ni(II) polynuclear complexes.[10] According to the theory of Hoffmann[27] and Kahn,[28] if we consider two interacting octahedral Ni(II) ions, the J parameter of the spin Hamiltonian can be decomposed into a ferromagnetic term (j_f), which depends on the two-electron integrals, and an antiferromagnetic term (J_{af}) which depends on the splitting of the pairs of MO's derived from d_{z^2} and d_{xy} respectively. Only when J_{af} is zero or negligible (orthogonal orbitals) may j_f be predominant and the behavior ferromagnetic. Extended Hückel calculation carried out on our dinuclear fragments clearly indicates that the gap between the highest and lowest orbitals is not negligible. While being mindful of the limitations of calculations of this kind, we may safely assume that in the present complexes there is no orthogonality which would lead to small values of J_{af} and hence that, on these grounds, the complex would be to expected to be antiferromagnetic. The ferromagnetism observed, however, can be readily explained by spin polarization effects, and hence, it may well be the key feature leading to ferromagnetism in our polynuclear Ni(II) complexes.

Acknowledgment. We are very grateful for the financial assistance from the CICYT (Grant No. PB90-0029) and to Dr. Michel Verdaguer (Université Piere et Marie Curie, Paris) and to Dr. Marc Drillon (EHICS, Strasbourg, France) for some of the magnetic measurements and a helpful discussion of the results.

Supplementary Material Available: Tables giving crystal data and details of the structure determination, anisotropic thermal parameters, hydrogen atom coordinates, and bond angles and distances (16 pages). Ordering information is given on any current masthead page.

(27) Hay, P. J.; Thibeault, J. C.; Hoffmann, R. *J. Am. Chem. Soc.* **1975**, *97*, 4884.
(28) (a) Kahn, O.; Briat, B. *J. Chem. Soc., Faraday Trans.* **1976**, *72*, 268. (b) Kahn, O.; Briat, B. *J. Chem. Soc., Faraday Trans.* **1976**, *72*, 1441. (c) Kahn, O.; Briat, B.; Galy, J. *J. Chem. Soc., Dalton Trans.* **1977**, 1453.